

Mind the Way You Select Negative Texts: Pursuing the Distance Consistency in OOD Detection with VLMs

Zhikang Xu^{1,2} Qianqian Xu^{3,*} Zitai Wang³ Cong Hua³
Sicong Li^{1,2} Zhiyong Yang⁴ Qingming Huang^{4,3,5,*}

¹Institute of Information Engineering, Chinese Academy of Sciences

²School of Cyber Security, University of Chinese Academy of Sciences

³State Key Laboratory of AI Safety, Institute of Computing Technology, Chinese Academy of Sciences

⁴School of Computer Science and Technology, University of Chinese Academy of Sciences

⁵BDKM, University of Chinese Academy of Sciences

{xuzhikang, lisicong}@iie.ac.cn {xuqianqian, wangzitai, huacong23z}@ict.ac.cn

{yangzhiyong21, qmhuang}@ucas.ac.cn

Abstract

*Out-of-distribution (OOD) detection seeks to identify samples from unknown classes, a critical capability for deploying machine learning models in open-world scenarios. Recent research has demonstrated that Vision-Language Models (VLMs) can effectively leverage their multi-modal representations for OOD detection. However, current methods often incorporate **intra-modal** distance during OOD detection, such as comparing negative texts with ID labels or comparing test images with image proxies. This design paradigm creates an inherent inconsistency against the **inter-modal** distance that CLIP-like VLMs are optimized for, potentially leading to suboptimal performance. To address this limitation, we propose InterNeg, a simple yet effective framework that systematically utilizes consistent inter-modal distance enhancement from textual and visual perspectives. From the textual perspective, we devise an inter-modal criterion for selecting negative texts. From the visual perspective, we dynamically identify high-confidence OOD images and invert them into the textual space, generating extra negative text embeddings guided by inter-modal distance. Extensive experiments across multiple benchmarks demonstrate the superiority of our approach. Notably, our InterNeg achieves state-of-the-art performance compared to existing works, with a 3.47% reduction in FPR95 on the large-scale ImageNet benchmark and a 5.50% improvement in AUROC on the challenging Near-OOD benchmark. Code will be available at <https://github.com/ZhikangXu0112/InterNeg>.*

1. Introduction

Most machine learning algorithms [25, 39, 40, 58, 72] are designed based on the closed-world assumption, where training and testing datasets share the same label space. However, in real-world applications, models inevitably encounter samples from unknown classes, which are referred to as *out-of-distribution* (OOD) data. In such scenarios, models often exhibit overconfidence, misclassifying OOD data into known classes [45], posing significant risks in high-stakes scenarios like risk content identification, autonomous driving, and medical diagnosis [4]. Consequently, OOD detection is crucial for building trustworthy and secure artificial intelligence systems and has garnered widespread attention [50, 67].

Traditional visual OOD detection methods [33, 36, 37, 60] focus on training powerful representation models and designing OOD scoring functions based on a single image modality. Recently, inspired by the power of vision-language models (VLMs) such as CLIP [47], an increasing number of studies [14, 16, 29, 41] have explored how to leverage the rich multi-modal knowledge to enhance OOD detection capabilities. Specifically, ZOC [14] and MCM [41] introduce zero-shot OOD detection, utilizing VLMs to identify OOD samples without the need for training on *in-distribution* (ID) data. NegLabel [29] proposes to mine massive negative texts that are semantically distant from ID labels in the textual space to further unlock the potential of VLMs in enhancing OOD detection performance. Owing to its simplicity and strong empirical performance, NegLabel has inspired a series of subsequent studies [6, 16, 74] that build upon its framework to advance the field of OOD detection further. Remarkably, these methods even outperform those [1, 35, 43, 46, 59] that require training on ID data.

*Corresponding authors

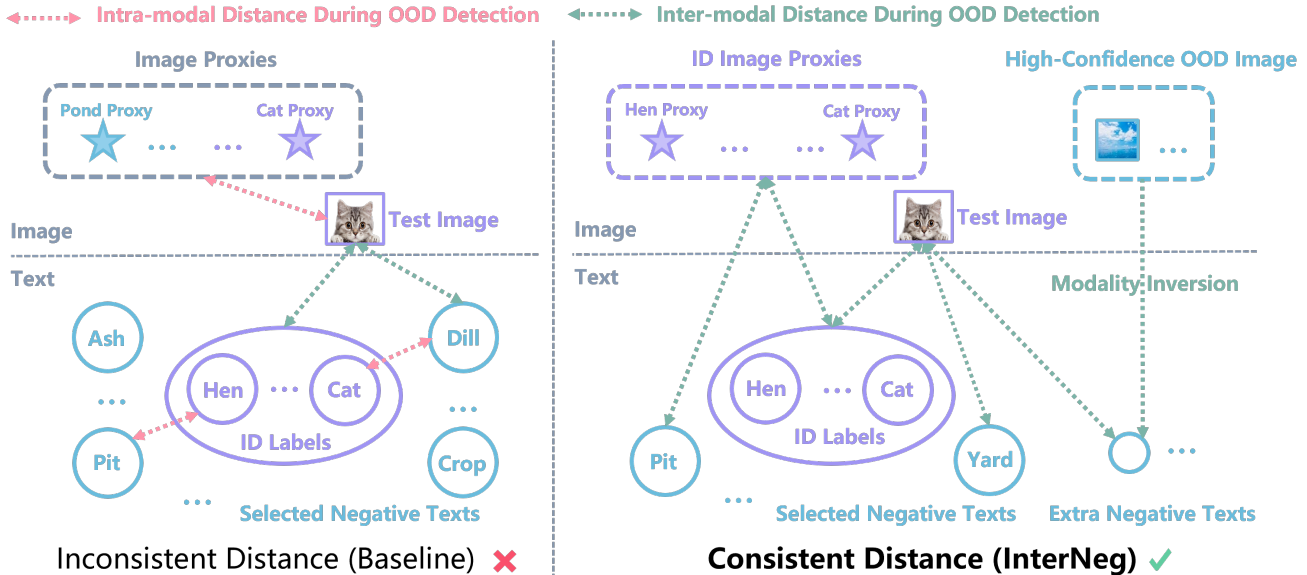


Figure 1. Comparison of Baseline and InterNeg. The baseline often incorporates **intra-modal** distance during OOD detection, which is inconsistent with the **inter-modal** distance that CLIP-like VLMs are optimized for. In contrast, InterNeg leverages consistent inter-modal distance during OOD detection, enhancing performance by inter-modal guided negative texts and extra negative text embeddings generated through modality inversion.

However, as shown in Figure 1, existing methods [29, 74] often adopt **intra-modal** (*i.e.* image-image and text-text) distance during OOD detection, by either comparing negative texts with ID labels or comparing test images with image proxies. This strategy contradicts the **inter-modal** (*i.e.* image-text) optimization objective of CLIP-style VLMs [42, 47], potentially resulting in suboptimal performance. For instance, while some negative texts have a large intra-modal distance from ID labels, their inter-modal distance to the ID test image may still be smaller than that of the ID labels to the ID test image, potentially causing ID misclassification. In Section 4.1, we provide a detailed analysis to further explain this issue.

To address this limitation, we introduce InterNeg, a simple yet effective approach that explicitly utilizes consistent inter-modal distance from textual and visual perspectives without requiring training on ID or extra data. **From the textual perspective**, we propose an inter-modal guided negative text selection strategy by introducing an ID inter-modal base distance. **From the visual perspective**, we leverage high-confidence OOD image inversion to generate extra negative text embeddings during inference. Since high-confidence OOD images are determined by a fixed threshold, some noisy samples may be inadvertently included. To mitigate this issue, we also introduce an inter-modal guided dynamic filtering mechanism. Finally, after obtaining the inter-modal guided negative texts and extra negative text embeddings, our method effectively achieves enhanced performance.

Extensive experimental results demonstrate that our method achieves state-of-the-art performance on various OOD detection benchmarks. Specifically, on the large-scale ImageNet-1K traditional Four-OOO benchmark [27], our approach yields a notable 3.47% reduction in FPR95 while improving AUROC by 0.77% over the existing methods. Moreover, on the more challenging Near-OOO benchmark [66, 73], our method achieves a substantial 2.09% reduction in FPR95 and a significant 5.50% improvement in AUROC. In summary, our main contributions can be listed as follows:

- To the best of our knowledge, we are the first to identify an inconsistency between the intra-modal distance during OOD detection and the inter-modal distance that CLIP-like VLMs are optimized for, which may lead to suboptimal performance.
- We propose InterNeg, a simple yet effective approach that leverages consistent inter-modal distance from both textual and visual perspectives without requiring training on any data.
- Extensive experiments on multiple benchmarks demonstrate that our method achieves state-of-the-art performance. Moreover, ablation studies and further discussions also validate the effectiveness and robustness of our method.

2. Related Work

Visual-based Traditional OOD Detection. Traditional OOD detection methods only use single image modal-

ity, which can be broadly categorized into score-based [20, 27, 32, 36, 37, 51, 56], density-based [48, 64], and distance-based [12, 52]. Score-based methods leverage a well-trained classifier to derive better score functions. Density-based methods model the ID data probabilistically, flagging samples in low-density regions as OOD. Distance-based methods detect OOD samples by measuring feature space distances to ID prototypes. However, these methods are based solely on the visual modality, overlooking the potential benefits that integrating the textual modality could bring.

VLM-based OOD Detection. Recently, the advent of powerful pre-trained vision-language models (VLMs), such as CLIP [47], has inspired a growing number of research leveraging VLMs for OOD detection. These works can be broadly divided into few-shot and zero-shot learning approaches. LoCoOp [43] first proposes few-shot OOD detection, extracting regions from the local features of CLIP that are irrelevant to the ID data as regularization constraints for OOD detection. A subsequent series of works [1, 18, 26, 35, 46, 59] have focused on training negative text prompts to identify OOD samples.

The zero-shot OOD detection task is first proposed by ZOC [14], which trains an unknown-class text generator. However, this approach yields poor results when dealing with large-scale ID datasets such as ImageNet-1K. MCM [41] introduces a temperature-scaled maximum softmax probability as the OOD detection score, yet this method solely relies on ID labels without fully leveraging the open-world textual capabilities of VLMs. To enrich textual information, CLIPN [57] trained an additional negative text encoder using auxiliary datasets, while NegLabel [29] selected numerous potential negative text labels from large lexical corpus (e.g., WordNet [15]) to approximate OOD labels. EOE [5] designed multi-granularity prompts based on image similarity and employed large language models to generate potential OOD labels. Among these, NegLabel has been widely adopted in subsequent works [6, 16, 74] due to its simplicity and efficiency. Building upon this foundation, CLIPScope [16] proposes a more robust OOD scoring method based on Bayesian theory, while CSP [6] theoretically demonstrates that expanding the corpus size enhances OOD detection capability and proposes a practical expansion approach. Meanwhile, AdaNeg [74] employs a memory bank during inference to store high-confidence samples, effectively aligning with OOD label space by generating adaptive negative proxies.

3. Preliminaries

Problem Setups. Let \mathcal{X}^{ID} and $\mathcal{Y}^{\text{ID}} = \{y_1, y_2, \dots, y_C\}$ be the ID image space and ID label space, where \mathcal{Y} consists text words like $\mathcal{Y}^{\text{ID}} = \{cat, dog, \dots, goose\}$ and C is the total

number of ID classes. In closed-world scenarios, it is assumed that the training and testing data come from the same distribution \mathcal{X}^{ID} . However, in real-world applications, models may inevitably encounter samples from unknown classes, denoted by $\mathbf{x} \in \mathcal{X}^{\text{OOD}}$ and $y \in \mathcal{Y}^{\text{OOD}}$. In such scenarios, models may misclassify OOD data into ID classes with high confidence [45]. To address this issue, OOD detection [67] is proposed to identify ID data and reject OOD data using a score function $S(\cdot)$ [20, 33, 36, 37]. Let $\mathcal{X} = \mathcal{X}^{\text{ID}} \cup \mathcal{X}^{\text{OOD}}$ and $\mathcal{X}^{\text{ID}} \cap \mathcal{X}^{\text{OOD}} = \emptyset$, given a test sample $\mathbf{x} \in \mathcal{X}$, the OOD detector $G(\cdot)$ can be defined as:

$$G_\gamma(\mathbf{x}) = \begin{cases} \text{ID}, & \text{if } S(\mathbf{x}) \geq \gamma; \\ \text{OOD}, & \text{otherwise,} \end{cases} \quad (1)$$

where $\gamma \in \mathbb{R}$ is a predefined threshold to distinguish ID/OOD classes. The test sample \mathbf{x} is detected as ID data if and only if $S(\mathbf{x}) \geq \gamma$.

CLIP-based VLMs. CLIP [47] is a foundational VLM pre-trained on 400 million image-text pairs collected from the internet using self-supervised contrastive learning. It contains a text encoder $\mathcal{T}(\cdot)$ using the Transformer [54] architecture and an image encoder $\mathcal{I}(\cdot)$ using the ViT [11] or ResNet [19] architecture. Given a batch of N image-text pairs $\{\mathbf{x}_i, y_i\}_{i=1}^N$, we extract the image features $\mathbf{h}_i \in \mathbb{R}^d$ and text features $\mathbf{e}_i \in \mathbb{R}^d$ as follows:

$$\mathbf{h}_i = \mathcal{I}(\mathbf{x}_i), \quad \mathbf{e}_i = \mathcal{T}(\mathcal{E}(\text{prompt}(y_i))), \quad \forall i = 1, 2, \dots, N, \quad (2)$$

where $\text{prompt}(\cdot)$ represents the prompt template for input labels, e.g., "a photo of [class]", $\mathcal{E}(\cdot)$ is word embedding function and d is the embedding dimension. During training, CLIP optimizes a symmetric contrastive loss that explicitly minimizes the **inter-modal** distance (i.e., cosine similarity) between matched image-text pairs while maximizing it for unmatched pairs:

$$\mathcal{L}_{\text{CLIP}} = -\frac{1}{N} \sum_{i=1}^N \left(\log \frac{e^{\cos(\mathbf{h}_i, \mathbf{e}_i)/\tau}}{\sum_{j=1}^N e^{\cos(\mathbf{h}_i, \mathbf{e}_j)/\tau}} + \log \frac{e^{\cos(\mathbf{e}_i, \mathbf{h}_i)/\tau}}{\sum_{j=1}^N e^{\cos(\mathbf{e}_i, \mathbf{h}_j)/\tau}} \right), \quad (3)$$

where $\cos(\cdot, \cdot)$ denotes the cosine similarity and τ is the temperature parameter. During inference, for a image $\mathbf{x} \in \mathcal{X}^{\text{ID}}$, $y \in \mathcal{Y}^{\text{ID}}$, the predictions are calculated by the cosine similarity between the image features \mathbf{h} and text features \mathbf{e}_i :

$$\hat{y} = \arg \max_{y_i \in \mathcal{Y}^{\text{ID}}} \text{softmax}\{\cos(\mathbf{h}, \mathbf{e}_i)\}. \quad (4)$$

The vanilla CLIP is proposed to perform zero-shot ID classification. Recently, it has been extended to zero-shot OOD detection.

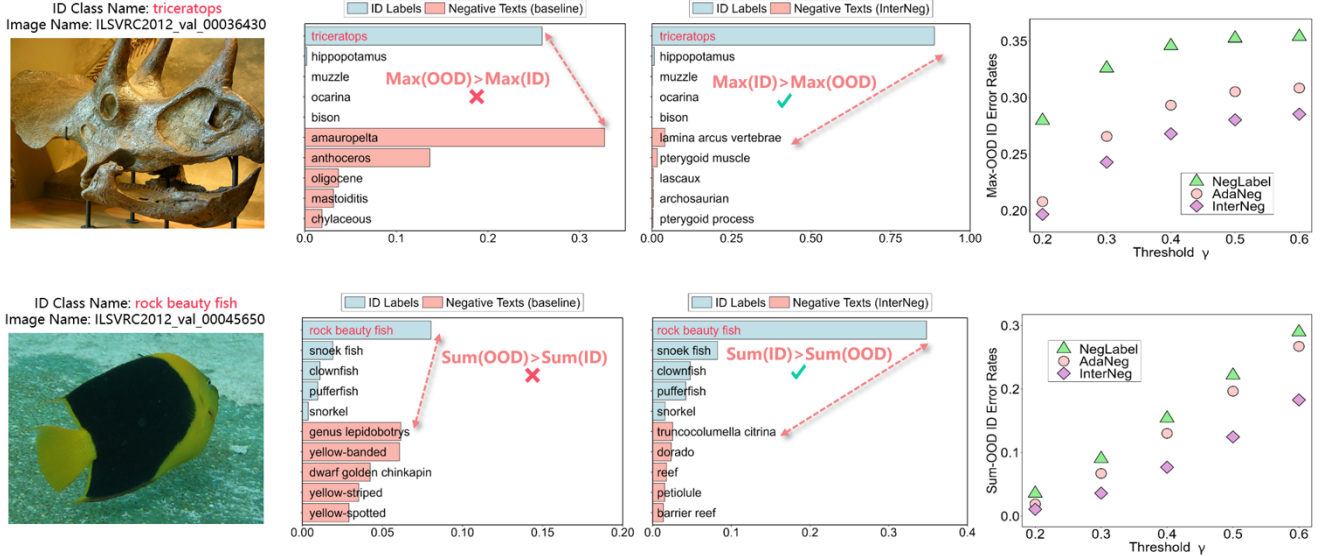


Figure 2. Two types of ID misclassification. *First Row*: Max-OOD dominant ID misclassification. *Second Row*: Sum-OOD dominant ID misclassification. *Left*: Original ID image from ImageNet-1K with its class label and filename. *Middle*: Top-5 softmax scores for ID labels and negative texts of baseline and our method. *Right*: Max-OOD/Sum-OOD dominant ID error rates under different thresholds γ of baseline and our method.

CLIP for OOD detection (NegLabel) [29]. As a straightforward and effective method, NegLabel has been widely used in recent works [6, 16, 74]. Specifically, NegLabel proposes to mine a set of negative texts $\mathcal{Y}^- = \{y_{C+1}, y_{C+2}, \dots, y_{C+M}\}$ from a large text corpus, where $\mathcal{Y}^- \cap \mathcal{Y}^{\text{ID}} = \emptyset$ and M is the number of selected negative texts. These negative texts are selected based on intra-modal distance, which means they exhibit lower cosine similarity with ID labels, thereby serving as an approximation for the true OOD labels. Then, we can extend the text features as ID label features e_i and negative text features $e_i^- \in \mathbb{R}^d$:

$$e_i^- = \mathcal{T}(\mathcal{E}(\text{prompt}(y_{i+C}))), \quad \forall i = 1, 2, \dots, M, \quad (5)$$

On top of this, NegLabel proposes an OOD score function to distinguish ID/OOD samples as follows:

$$S_{\text{NegLabel}}(\mathbf{x}) = \frac{\sum_{i=1}^C e^{\cos(\mathbf{h}, \mathbf{e}_i)/\tau}}{\sum_{i=1}^C e^{\cos(\mathbf{h}, \mathbf{e}_i)/\tau} + \sum_{i=1}^M e^{\cos(\mathbf{h}, \mathbf{e}_i^-)/\tau}}, \quad (6)$$

where $\tau > 0$ is the scaling temperature. In a word, NegLabel extends the label space to fully leverage the potential of utilizing VLMs for OOD detection.

4. Methodology

4.1. Motivations

Existing approaches, such as NegLabel and AdaNeg, utilize intra-modal distance during OOD detection. However, large

intra-modal distances do not guarantee correspondingly large inter-modal distances, potentially leading to ID misclassification (*i.e.*, misclassifying ID as OOD). In Figure 2, we visualize the results of two ID images in the ImageNet-1K dataset and identify two distinct types of ID misclassification:

- **Max-OOD dominant** occurs when the highest-scoring negative (OOD) text surpasses the score of the highest-scoring in-distribution (ID) label, leading to ID misclassification. For instance, if the selected negative text "Amauropelta" receives a higher score than the ground-truth label "Triceratops," the ID input is misclassified.
- **Sum-OOD dominant** refers to cases where the total negative text score exceeds the total ID score, excluding cases already categorized as Max-OOD. For instance, the prior arts may select negative texts such as "genus lepidobotrys", "yellow-banded", "dwarf golden chinkapin", and so on. Although none of these individually dominate, their aggregated score surpasses that of the ground-truth label, ultimately leading to the misclassification of the ID input.

To quantify these phenomena, we compute the ID error rates for Max-OOD and Sum-OOD cases under varying threshold values γ , comparing baseline methods and our proposed approach under an equal number of negative texts. The results highlight the limitations of existing methods, whereas our consistent inter-modal based method effectively mitigates these issues. More results can be found in Appendix B.6.

4.2. InterNeg: Inter-modal Guided OOD Detection

To ensure the distance consistency in OOD detection with CLIP-like VLMs, we propose InterNeg, a simple yet effective method that utilizes consistent inter-modal distance from textual and visual perspectives without requiring training on ID or extra data.

4.2.1. Inter-modal Guided Negative Text Selection

From the textual perspective, we introduce an inter-modal guided strategy for negative text selection. To compute the inter-modal distance, we first need to obtain ID image proxies. Intuitively, we randomly sample N ID images per class from the training set and encode them using the CLIP image encoder $\mathcal{I}(\cdot)$ to obtain their embeddings. Subsequently, we compute the class-wise mean embeddings as ID image proxies \mathbf{p}_i :

$$\mathbf{p}_i = \frac{1}{N} \sum_{j=1}^N \mathcal{I}(\mathbf{x}_{ij}), \quad i = 1, 2, \dots, C, \quad (7)$$

where \mathbf{x}_{ij} denotes the j -th sample in the i -th ID class. We then define the **ID inter-modal base distance** for each class with ID text proxies \mathbf{e}_i :

$$d_i^{\text{base}} = 1 - \cos(\mathbf{e}_i, \mathbf{p}_i), \quad i = 1, 2, \dots, C, \quad (8)$$

Next, we consider using d_i^{base} to select negative texts. Given a text y from a large-scale corpus database WordNet [15], we first compute the inter-modal distance with ID image proxies:

$$\begin{aligned} \mathbf{e}^y &= \mathcal{T}(\mathcal{E}(\text{prompt}(y))), \\ d_i(\mathbf{e}^y) &= 1 - \cos(\mathbf{e}^y, \mathbf{p}_i), \quad i = 1, 2, \dots, C, \end{aligned} \quad (9)$$

where $d_i(\mathbf{e}^y)$ denotes the inter-modal distance for text y of the i -th class and $\mathcal{E}(\cdot)$ is the word embedding function.

Intuitively, to select texts that effectively discriminate against ID labels, we choose those that satisfy $\forall i, d_i(\mathbf{e}^y) > d_i^{\text{base}}$ as candidate texts. We refer to such texts as **inter-modal guided negative texts**. This criterion guarantees that inter-modal guided negative texts maintain large distances from all class-wise ID image-text pairs, improving their ability to approximate true OOD labels. Lastly, the negative set \mathcal{Y}^- is formed by selecting the top- M candidates with the highest **deviation degree**, which quantifies the discriminative capability of each negative text:

$$D(\mathbf{e}^y) = \sum_{i=1}^C d_i(\mathbf{e}^y) - d_i^{\text{base}}, \quad (10)$$

Consequently, the negative texts selected above ensure consistency with the inter-modal optimization goal of CLIP-style VLMs are optimized for, further enhancing OOD detection performance.

Algorithm 1 InterNeg

Require: ID label space \mathcal{Y}^{ID} and test dataset \mathcal{X} ;

- 1: Select top- M inter-modal guided negative texts \mathcal{Y}^- based on \mathcal{Y}^{ID} in Section 4.2.1;
 - 2: Initialize an empty extra negative text embeddings set \mathcal{N}^- ;
 - 3: **for** $x \in \mathcal{X}$ **do**
 - 4: Calculate the OOD score $S(x)$ using Eq.(11) ;
 - 5: **if** $S(x) \leq \beta$ **then**
 - 6: ▷ **Step 1: Generating Extra Negative Text Embeddings**
 - 7: Invert high-confidence OOD images to generate extra negative text embedding \mathbf{e}_v^- ;
 - 8: ▷ **Step 2: Filtering Extra Negative Text Embeddings**
 - 9: **if** $\forall i, d_i(\mathbf{e}_v^-) > d_i^{\text{base}}$ **then**
 - 10: Add \mathbf{e}_v^- to the set \mathcal{N}^- and record the deviation degree using Eq.(10);
 - 11: **if** $|\mathcal{N}^-| > K$ **then**
 - 12: Only retain the top- K text embeddings in set \mathcal{N}^- based on the deviation degrees;
 - 13: **end if**
 - 14: Compute the final OOD score S_{final} again using Eq.(11) ;
 - 15: **end if**
 - 16: **end if**
 - 17: **end for**
 - 18: **return** Collect all the OOD scores S_{final} .
-

4.2.2. Inter-modal Guided Extra Negative Texts

From the visual perspective, we dynamically leverage OOD images to enhance the negative textual space through inter-modal distance during inference. To obtain these OOD images, we use test samples that are classified as OOD with high confidence. These high-confidence OOD images are then inverted into the textual space to produce extra negative text embeddings. Formally, let \mathcal{N}^- represent the set of extra negative text embeddings, where $|\mathcal{N}^-|$ denotes the number of embeddings in the set. The enhanced OOD score function is then defined as follows:

$$S(\mathbf{x}) = \left(\sum_{i=1}^C e^{\cos(\mathbf{h}, \mathbf{e}_i)/\tau} \right) \left(\underbrace{\sum_{i=1}^C e^{\cos(\mathbf{h}, \mathbf{e}_i)/\tau}}_{\text{ID Labels}} + \underbrace{\sum_{i=1}^M e^{\cos(\mathbf{h}, \mathbf{e}_i^-)/\tau}}_{\text{Selected Negative Texts}} + \underbrace{\sum_{\mathbf{e}_v^- \in \mathcal{N}^-} e^{\cos(\mathbf{h}, \mathbf{e}_v^-)/\tau}}_{\text{Extra Negative Text Embeddings}} \right)^{-1}, \quad (11)$$

where \mathbf{e}_v^- denotes the extra negative text embedding, whose details are described below. Initially, \mathcal{N}^- is set to be empty. During inference, our method dynamically expands \mathcal{N}^-

Table 1. OOD detection results with ID dataset of ImageNet-1k and traditional Four-OOD datasets using CLIP ViT-B/16 architecture. \uparrow indicates larger values are better and \downarrow indicates smaller values are better. All values are percentages with **bold** and underline indicating the best and second-best results, respectively.

Methods	OOD Datasets								Average	
	iNaturalist		SUN		Places		Textures		AUROC \uparrow	FPR95 \downarrow
	AUROC \uparrow	FPR95 \downarrow								
Visual-based Methods (requiring training on ID or extra data)										
MSP [20]	87.44	58.36	79.73	73.72	79.67	74.41	79.69	71.93	81.63	69.61
ODIN [36]	94.65	30.22	87.17	54.04	85.54	55.06	87.85	51.67	88.80	47.75
Energy [37]	95.33	26.12	92.66	35.97	91.41	39.87	86.76	57.61	91.54	39.89
GradNorm [28]	72.56	81.50	72.86	82.00	73.70	80.41	70.26	79.36	72.35	80.82
ViM [56]	93.16	32.19	87.19	54.01	83.75	60.67	87.18	53.94	87.82	50.20
KNN [52]	94.52	29.17	92.67	35.62	91.02	39.61	85.67	64.35	90.97	42.19
VOS [13]	94.62	28.99	92.57	36.88	91.23	38.39	86.33	61.02	91.19	41.32
VLM-based Methods (requiring training on ID or extra data)										
LoCoOp [43]	96.86	16.05	95.07	23.44	91.98	32.87	90.19	42.28	93.52	28.66
LSN [46]	95.83	21.56	94.35	26.32	91.25	34.48	90.42	38.54	92.96	30.22
ID-Like [1]	98.19	8.98	91.64	42.03	90.57	44.00	94.32	<u>25.27</u>	93.68	30.07
NegPrompt [35]	98.73	6.32	95.55	22.89	93.34	27.60	91.60	35.21	94.81	23.01
SUPREME [59]	98.29	8.27	95.84	19.40	93.56	26.69	94.45	26.77	95.54	20.28
Local-Prompt [70]	98.07	8.63	95.12	23.23	92.42	31.74	92.29	34.50	94.48	24.52
ZOC [14]	86.09	87.30	81.20	81.51	83.39	73.06	76.46	98.90	81.79	85.19
CLIPN [57]	95.27	23.94	93.93	26.17	92.28	33.45	90.93	40.83	93.10	31.10
LAPT [75]	99.63	1.16	96.01	19.12	92.01	33.01	91.06	40.32	94.68	23.40
VLM-based Zero-Shot Methods (no training on ID or extra data)										
Mahalanobis [32]	55.89	99.33	59.94	99.41	65.96	98.54	64.23	98.46	61.50	98.94
Energy [37]	85.09	81.08	84.24	79.02	83.38	75.08	65.56	93.65	79.57	82.21
MCM [41]	94.59	32.20	92.25	38.80	90.31	46.20	86.12	58.50	90.82	43.93
EOE [5]	97.52	12.29	95.73	20.40	92.95	30.16	85.64	57.53	92.96	30.09
NegLabel [29]	99.49	1.91	95.49	20.53	91.64	35.59	90.22	43.56	94.21	25.40
CLIPScope [16]	99.61	1.29	96.77	15.56	93.54	28.45	91.41	38.37	95.30	20.88
CoVer [71]	95.98	22.55	93.42	32.85	90.27	40.71	90.14	43.39	92.45	34.88
CSP [6]	99.60	1.54	96.66	13.66	92.90	29.32	93.86	25.52	95.76	<u>17.51</u>
AdaNeg [74]	99.71	<u>0.59</u>	<u>97.44</u>	<u>9.50</u>	<u>94.55</u>	34.34	<u>94.93</u>	31.27	96.66	18.92
InterNeg	99.79	0.40	98.68	6.78	95.01	<u>27.11</u>	96.26	21.85	97.43	14.04

through an iterative two-step process.

Step 1: Generating Extra Negative Text Embeddings. If $S(\mathbf{x}) \leq \beta$, the image \mathbf{x} is identified as a high-confidence OOD image, where β is a hyperparameter serving as the threshold for this determination. To obtain the negative text embeddings, we use the modality inversion technique in [2, 42] to transform the above high-confidence OOD images into textual space. Specifically, for a high-confidence OOD image \mathbf{x} , we first randomly initialize a set of T pseudo-tokens $\mathbf{v} = \{v_1, v_2, \dots, v_T\}$ and concatenate with the text template (e.g., "a photo of") to form $\bar{\mathbf{v}} = [\mathcal{E}(\text{"a photo of"}), \mathbf{v}]$. Then, we extract the image embedding \mathbf{h} and text embedding e_v^- and as follows:

$$e_v^- = \mathcal{T}(\bar{\mathbf{v}}), \quad \mathbf{h} = \mathcal{I}(\mathbf{x}) \quad (12)$$

Next, we optimize \mathbf{v} through minimizing the cosine distance loss between the image and text embeddings $\mathcal{L} =$

$1 - \cos(e_v^-, \mathbf{h})$, which is based on the inter-modal distance. Hence, **we get an extra negative text embedding** e_v^- . Please refer to Algorithm 2 for the pseudo-code of the modality inversion process.

Step 2: Filtering Extra Negative Text Embeddings.

Since a fixed threshold is applied above, some noisy images may be incorrectly included. To mitigate these noisy images, we implement an **inter-modal guided dynamic filtering mechanism**. On one hand, we also leverage an **inter-modal guided selection** for the generated negative text embeddings. Specifically, we utilize the extra negative text embedding e_v^- to calculate $d_i(e_v^-)$ and compare with d_i^{base} (as described in Section 4.2.1). Only those e_v^- that satisfy $\forall i, d_i(e_v^-) > d_i^{\text{base}}$ are added to \mathcal{N}^- with their corresponding deviation degrees $D(e_v^-)$, others are discarded. On the other hand, we **limit the size of the extra negative text embeddings set** \mathcal{N}^- to a maximum of K , where K is

Table 2. OOD detection results with ID dataset of ImageNet-1k and OpenOOD benchmark using CLIP ViT-B/16 architecture. Full results are available in Table 4.

Methods	FPR95 ↓		AUROC ↑	
	Near-OOD	Far-OOD	Near-OOD	Far-OOD
Methods requiring training on ID or extra data				
GEN [38]	–	–	78.97	90.98
ReAct [51]	–	–	79.94	93.70
RMDS [49]	–	–	80.09	92.60
SCALE [65]	–	–	81.36	96.53
ASH [10]	–	–	82.16	96.05
LAPT [75]	58.94	24.86	82.63	94.26
Zero-shot methods (no training on ID or extra data)				
MCM [41]	79.02	68.54	60.11	84.77
NegLabel [29]	69.45	23.73	75.18	94.85
AdaNeg [74]	67.51	17.31	76.70	96.43
InterNeg	65.43	16.96	82.20	96.71

a hyperparameter. Specifically, when the addition of new embeddings causes $|\mathcal{N}^-|$ to exceed K , we sort all embeddings in \mathcal{N}^- by their deviation degrees and retain only the top- K highest-scoring ones, discarding the rest. The overall pipeline of our method is summarized in Algorithm 1.

5. Experiments

5.1. Main Results

OOD Detection Performance Comparison on Traditional Four-OOD Datasets. In Table 1, we compare our proposed method with other existing OOD detection methods. Specifically, we report the traditional visual-based methods from MSP [20] to VOS, and recent VLM-based methods from LoCoOp [43] to AdaNeg [74]. The experimental results demonstrate that our proposed method achieves state-of-the-art performance, significantly outperforming the closest baseline with substantial improvements of 0.77% in AUROC and 3.47% in FPR95, thereby validating the effectiveness and superiority of our method.

OOD Detection Performance Comparison on OpenOOD Setup.

Following [74], we also evaluate our method on the OpenOOD benchmark, which contains challenging Near-OOD and easy Far-OOD datasets. Referred from [66, 73, 74], we report the results of zero-shot methods and methods requiring training on ID or extra data in Table 2. Based on the experimental results, our proposed method demonstrates consistent superiority over existing zero-shot approaches across both Near-OOD and Far-OOD scenarios. Notably, in Near-OOD scenarios, our approach achieves significant improvements with a 5.50% increase in AUROC and a 2.09% reduction in FPR95. These substantial enhancements make our method competitive with approaches that require training on any data.

Table 3. Ablation study. Average results on the Four-OOD benchmark, where SNT denotes Selected Negative Texts and ENT denotes Extra Negative Text embeddings, both of which can be obtained by Intra-modal or Inter-modal distances.

Intra SNT	Inter SNT	Intra ENT	Inter ENT	AUROC ↑	FPR95 ↓
✓				94.21	25.40
	✓			94.56	24.12
✓		✓		95.89	20.84
	✓	✓		96.22	19.99
✓			✓	97.11	14.76
	✓		✓	97.43	14.04

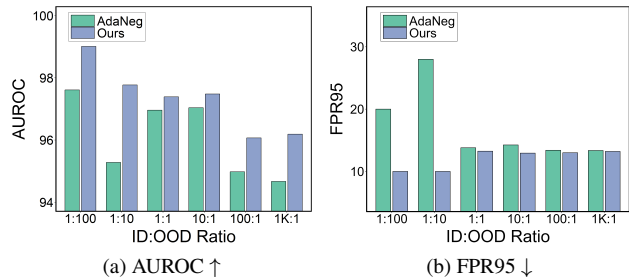


Figure 3. AUROC ↑ and FPR95 ↓ average performance under varying ID:OOD ratios.

5.2. Ablation Study and Discussion

Ablation on Each Module in InterNeg. Table 3 presents a comprehensive ablation study comparing our proposed method with four alternative approaches to validate its effectiveness: (1) Intra SNT, this baseline utilizes negative texts selected by intra-modal distance in NegLabel [29]. (2) Inter SNT, it represents the first component of our proposed method (Section 4.2.1), employing inter-modal guided negative texts. (3) Intra SNT + Intra ENT, a variant where both components of our method are replaced with intra-modal distance. The selected negative texts are intra-modal guided, and extra negative text embeddings are filtered using intra-modal distance. (4) Inter SNT + Intra ENT, a hybrid approach that uses our inter-modal guided negative texts selection but employs intra-modal distance for filtering extra negative text embeddings. (5) Intra SNT + Inter ENT, a hybrid approach combining NegLabel with our proposed inter-modal guided extra negative text embeddings. The experimental results demonstrate the superior performance of both components in our method (Inter SNT + Inter ENT).

Imbalanced ID and OOD Test Data. To evaluate our method under imbalanced ID and OOD test settings [17, 34, 61, 62, 68, 69, 76], we construct datasets with varying ID:OOD ratios. Specifically, we first create four basic configurations by: (1) randomly selecting 1K samples from the SUN dataset as OOD samples, and (2) independently sampling 10, 100, 1K, and 10K images from the ImageNet-1K

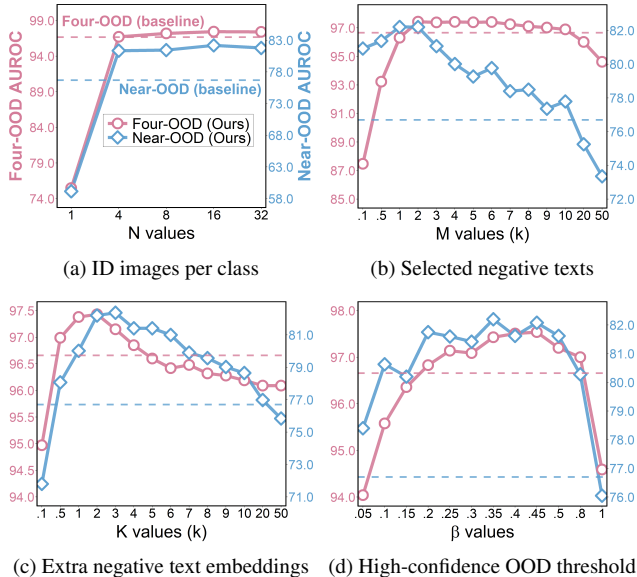


Figure 4. Parameter sensitivity analysis of four key hyperparameters: the number of ID images per class N , the number of selected negative texts M , the maximum size of extra negative text embeddings set K , and the high-confidence OOD threshold β , evaluated on both Four-OOD and Near-OOD benchmarks using ImageNet-1K as the ID dataset.

dataset as ID samples. This procedure yields ID:OOD ratios of 1:100, 1:10, 1:1, and 10:1 respectively. For more extreme ratios, we generate additional configurations by: (1) selecting only 10 samples from the SUN dataset as OOD data, and (2) pairing them with 1K or 1K ImageNet-1K samples to achieve ID:OOD ratios of 100:1 and 1K:1. All experimental data are drawn from Four-OOD benchmark to ensure no overlap between ID and OOD samples.

As shown in Figure 3, we compare our method with the best baseline AdaNeg (with adaptive gap strategy). Notably, even under highly imbalanced ID/OOD data distributions, our approach consistently outperforms AdaNeg by a substantial margin. This performance gap validates that our inter-modal guided dynamic filtering mechanism effectively mitigates the noise introduced by the fixed threshold, thereby confirming the robustness and reliability of our proposed method.

Further analyses regarding ID/OOD dataset ordering, various CLIP architectures, cross-domain settings, inference cost, and sensitivity to corpus choice are provided in Appendix B.

5.3. Parameter Sensitivity Analysis

The Number of ID images Per Class N . To examine the impact of the number of ID images per class serving as image proxies, we present the analysis in Figure 4a. The results demonstrate that using only one image per class yields

suboptimal performance, primarily because a single image may not sufficiently represent the class as an effective proxy. However, when the number of images per class reaches or exceeds 4 ($N \geq 4$), our method achieves state-of-the-art performance compared to the closest baseline. This finding indicates that our method requires only a small number of ID images per class to serve as effective image proxies. In all experiments, we choose $N = 16$ since it achieves optimal performance.

Selected Negative Texts Number M . As demonstrated in Figure 4b, our method achieves consistent and superior performance over all baselines across a broad spectrum of M values, highlighting its robustness. Empirical results indicate that optimal performance is achieved with a moderate number (e.g., $2000 \leq M \leq 9000$) of the selected negative texts. Based on this analysis, we set $M = 2000$ in all subsequent experiments.

Maximum Size of Extra Negative Text Embeddings Set K . As illustrated in Figure 4c, the model achieves optimal performance when the K value approaches the predefined number of selected negative texts ($M = 2000$). Beyond this point, performance gradually degrades as K increases, which can be attributed to the fixed threshold permitting more potentially erroneous OOD samples to be included in the consideration. Thus, we adopt $K = 2000$ throughout our experiments as it provides optimal performance for both Four-OOD and Near-OOD benchmarks.

High-confidence OOD Threshold β . As shown in Figure 4d, our method maintains robust performance across a wide range of β values, further validating the effectiveness of the inter-modal guided dynamic filtering mechanism. Since we choose $K = 2000$, even for larger β values, our approach selectively retains only the top- K most consistent negative text embeddings, ensuring stable and effective performance. Hence, we choose a moderate value of $\beta = 0.35$ for all experiments.

6. Conclusion

In this paper, we present InterNeg, a simple yet effective approach that improves OOD detection through consistent inter-modal distance without requiring training on ID or extra data. On one hand, we conduct an inter-modal guided negative text selection from the textual space. On the other hand, we utilize inter-modal guided high-confidence OOD images inversion to generate extra negative text embeddings from the visual space. Extensive experiments across diverse benchmarks demonstrate that InterNeg consistently achieves state-of-the-art performance, confirming our proposed method’s effectiveness and robustness.

Acknowledgement

This work was supported in part by National Natural Science Foundation of China: 62525212, U23B2051, 62236008, 62441232, 62521007, 62502500, 62576332, and U21B2038, in part by Youth Innovation Promotion Association CAS, in part by the Strategic Priority Research Program of the Chinese Academy of Sciences, Grant No. XDB0680201, in part by the project ZR2025ZD01 supported by Shandong Provincial Natural Science Foundation, in part by the China National Postdoctoral Program for Innovative Talents under Grant BX20240384, in part by Beijing Natural Science Foundation under Grant No. L252144, and in part by General Program of the Chinese Postdoctoral Science Foundation under Grant No. 2025M771558.

References

- [1] Yichen Bai, Zongbo Han, Bing Cao, Xiaoheng Jiang, Qinghua Hu, and Changqing Zhang. Id-like prompt learning for few-shot out-of-distribution detection. In *Conference on Computer Vision and Pattern Recognition*, pages 17480–17489, 2024. 1, 3, 6
- [2] Alberto Baldrati, Lorenzo Agnolucci, Marco Bertini, and Alberto Del Bimbo. Zero-shot composed image retrieval with textual inversion. In *International Conference on Computer Vision*, pages 15292–15301, 2023. 6
- [3] Julian Bitterwolf, Maximilian Müller, and Matthias Hein. In or out? fixing imagenet out-of-distribution detection evaluation. In *International Conference on Machine Learning*, pages 2471–2506, 2023. 1, 5
- [4] Rishi Bommasani, Drew A. Hudson, Ehsan Adeli, Russ B. Altman, Simran Arora, Sydney von Arx, Michael S. Bernstein, Jeannette Bohg, Antoine Bosselut, and Emma Brunskill et al. On the opportunities and risks of foundation models. *CoRR*, 2021. 1
- [5] Chentao Cao, Zhun Zhong, Zhanke Zhou, Yang Liu, Tongliang Liu, and Bo Han. Envisioning outlier exposure by large language models for out-of-distribution detection. In *International Conference on Machine Learning*, 2024. 3, 6
- [6] Mengyuan Chen, Junyu Gao, and Changsheng Xu. Conjugated semantic pool improves OOD detection with pre-trained vision-language models. In *Annual Conference on Neural Information Processing Systems*, pages 82560–82593, 2024. 1, 3, 4, 6, 5
- [7] Mircea Cimpoi, Subhansu Maji, Iasonas Kokkinos, Sammy Mohamed, and Andrea Vedaldi. Describing textures in the wild. In *Conference on Computer Vision and Pattern Recognition*, pages 3606–3613, 2014. 1, 2, 3, 5
- [8] Jia Deng, Wei Dong, Richard Socher, Li-Jia Li, Kai Li, and Li Fei-Fei. Imagenet: A large-scale hierarchical image database. In *Conference on Computer Vision and Pattern Recognition*, pages 248–255, 2009. 5
- [9] Li Deng. The mnist database of handwritten digit images for machine learning research [best of the web]. *IEEE signal processing magazine*, 29(6):141–142, 2012. 2, 3
- [10] Andrija Djuricic, Nebojsa Bozanic, Arjun Ashok, and Rosanne Liu. Extremely simple activation shaping for out-of-distribution detection. In *International Conference on Learning Representations*, pages 1–22, 2023. 7
- [11] Alexey Dosovitskiy, Lucas Beyer, Alexander Kolesnikov, Dirk Weissenborn, Xiaohua Zhai, Thomas Unterthiner, Mostafa Dehghani, Matthias Minderer, Georg Heigold, Sylvain Gelly, Jakob Uszkoreit, and Neil Houlsby. An image is worth 16x16 words: Transformers for image recognition at scale. In *International Conference on Learning Representations*, pages 1–22, 2021. 3, 5
- [12] Xuefeng Du, Gabriel Gozum, Yifei Ming, and Yixuan Li. SIREN: shaping representations for detecting out-of-distribution objects. In *Annual Conference on Neural Information Processing Systems*, pages 20434–20449, 2022. 3
- [13] Xuefeng Du, Zhaoning Wang, Mu Cai, and Yixuan Li. VOS: learning what you don’t know by virtual outlier synthesis. In *International Conference on Learning Representations*, pages 1–21, 2022. 6, 2
- [14] Sepideh Esmaeilpour, Bing Liu, Eric Robertson, and Lei Shu. Zero-shot out-of-distribution detection based on the pre-trained model CLIP. In *AAAI Conference on Artificial Intelligence*, pages 6568–6576, 2022. 1, 3, 6
- [15] Christiane Fellbaum. *WordNet: An Electronic Lexical Database*. Bradford Books, 1998. 3, 5
- [16] Hao Fu, Naman Patel, Prashanth Krishnamurthy, and Farshad khorrami. Clipse: Enhancing zero-shot ood detection with bayesian scoring. In *Proceedings of the Winter Conference on Applications of Computer Vision (WACV)*, pages 5346–5355, 2025. 1, 3, 4, 6, 5
- [17] Boyu Han, Qianqian Xu, Zhiyong Yang, Shilong Bao, Peisong Wen, Yangbangyan Jiang, and Qingming Huang. Aucseg: Auc-oriented pixel-level long-tail semantic segmentation. In *Annual Conference on Neural Information Processing Systems*, pages 126863–126907, 2024. 7
- [18] Boyu Han, Qianqian Xu, Shilong Bao, Zhiyong Yang, Kangli Zi, and Qingming Huang. Lightfair: Towards an efficient alternative for fair t2i diffusion via debiasing pre-trained text encoders. In *Annual Conference on Neural Information Processing Systems*, 2025. 3
- [19] Kaiming He, Xiangyu Zhang, Shaoqing Ren, and Jian Sun. Deep residual learning for image recognition. In *Conference on Computer Vision and Pattern Recognition*, pages 770–778, 2016. 3
- [20] Dan Hendrycks and Kevin Gimpel. A baseline for detecting misclassified and out-of-distribution examples in neural networks. In *International Conference on Learning Representations*, pages 1–12, 2017. 3, 6, 7, 2
- [21] Dan Hendrycks, Mantas Mazeika, and Thomas G. Dietterich. Deep anomaly detection with outlier exposure. In *International Conference on Learning Representations*, pages 1–18, 2019. 2
- [22] Dan Hendrycks, Mantas Mazeika, Saurav Kadavath, and Dawn Song. Using self-supervised learning can improve model robustness and uncertainty. In *Annual Conference on Neural Information Processing Systems*, pages 15637–15648, 2019. 2

- [23] Dan Hendrycks, Andy Zou, Mantas Mazeika, Leonard Tang, Bo Li, Dawn Song, and Jacob Steinhardt. Pixmix: Dreamlike pictures comprehensively improve safety measures. In *Conference on Computer Vision and Pattern Recognition*, pages 16762–16771, 2022. 2
- [24] Grant Van Horn, Oisín Mac Aodha, Yang Song, Yin Cui, Chen Sun, Alexander Shepard, Hartwig Adam, Pietro Perona, and Serge J. Belongie. The inaturalist species classification and detection dataset. In *Conference on Computer Vision and Pattern Recognition*, page 8769–8778, 2018. 1, 5
- [25] Cong Hua, Qianqian Xu, Shilong Bao, Zhiyong Yang, and Qingming Huang. Reconboost: Boosting can achieve modality reconciliation. In *International Conference on Machine Learning*, pages 19573–19597, 2024. 1
- [26] Cong Hua, Qianqian Xu, Zhiyong Yang, Zitai Wang, Shilong Bao, and Qingming Huang. Openworldauc: Towards unified evaluation and optimization for open-world prompt tuning. In *International Conference on Machine Learning*, pages 24975–25020, 2025. 3
- [27] Rui Huang and Yixuan Li. MOS: towards scaling out-of-distribution detection for large semantic space. In *Conference on Computer Vision and Pattern Recognition*, pages 8710–8719, 2021. 2, 3, 5
- [28] Rui Huang, Andrew Geng, and Yixuan Li. On the importance of gradients for detecting distributional shifts in the wild. In *Annual Conference on Neural Information Processing Systems*, pages 677–689, 2021. 6
- [29] Xue Jiang, Feng Liu, Zhen Fang, Hong Chen, Tongliang Liu, Feng Zheng, and Bo Han. Negative label guided OOD detection with pretrained vision-language models. In *International Conference on Learning Representations*, pages 1–29, 2024. 1, 2, 3, 4, 6, 7, 5
- [30] Alex Krizhevsky. Learning multiple layers of features from tiny images. 2009. 1, 2, 3
- [31] Ya Le and Xuan S. Yang. Tiny imagenet visual recognition challenge. 2015. 1, 2, 3
- [32] Kimin Lee, Kibok Lee, Honglak Lee, and Jinwoo Shin. A simple unified framework for detecting out-of-distribution samples and adversarial attacks. In *Annual Conference on Neural Information Processing Systems*, pages 7167–7177, 2018. 3, 6
- [33] Jingyao Li, Pengguang Chen, Zexin He, Shaozuo Yu, Shu Liu, and Jiaya Jia. Rethinking out-of-distribution (OOD) detection: Masked image modeling is all you need. In *IEEE/CVF Conference on Computer Vision and Pattern Recognition*, pages 11578–11589, 2023. 1, 3
- [34] Sicong Li, Qianqian Xu, Zhiyong Yang, Zitai Wang, Linchao Zhang, Xiaochun Cao, and Qingming Huang. Focal-sam: Focal sharpness-aware minimization for long-tailed classification. In *International Conference on Machine Learning*, pages 36624–36651, 2025. 7
- [35] Tianqi Li, Guansong Pang, Xiao Bai, Wenjun Miao, and Jin Zheng. Learning transferable negative prompts for out-of-distribution detection. In *Conference on Computer Vision and Pattern Recognition*, pages 17584–17594, 2024. 1, 3, 6
- [36] Shiyu Liang, Yixuan Li, and R. Srikant. Enhancing the reliability of out-of-distribution image detection in neural networks. In *International Conference on Learning Representations*, pages 1–15, 2018. 1, 3, 6
- [37] Weitang Liu, Xiaoyun Wang, John D. Owens, and Yixuan Li. Energy-based out-of-distribution detection. In *Annual Conference on Neural Information Processing Systems*, pages 21464–21475, 2020. 1, 3, 6, 2
- [38] Xixi Liu, Yaroslava Lochman, and Christopher Zach. GEN: pushing the limits of softmax-based out-of-distribution detection. In *Conference on Computer Vision and Pattern Recognition*, pages 23946–23955, 2023. 7, 2
- [39] Tianhao Ma, Han Chen, Juncheng Hu, Yungang Zhu, and Ximing Li. Forming auxiliary high-confident instance-level loss to promote learning from label proportions. In *Conference on Computer Vision and Pattern Recognition*, pages 20592–20601, 2025. 1
- [40] Tianhao Ma, Wei Wang, Ximing Li, Gang Niu, and Masashi Sugiyama. Learning from label proportions via proportional value classification. In *International Conference on Learning Representations*, pages 1–26, 2026. 1
- [41] Yifei Ming, Ziyang Cai, Jiuxiang Gu, Yiyou Sun, Wei Li, and Yixuan Li. Delving into out-of-distribution detection with vision-language representations. In *Annual Conference on Neural Information Processing Systems*, pages 35087–35102, 2022. 1, 3, 6, 7, 2
- [42] Marco Mistretta, Alberto Baldrati, Lorenzo Agnolucci, Marco Bertini, and Andrew D. Bagdanov. Cross the gap: Exposing the intra-modal misalignment in clip via modality inversion. In *International Conference on Learning Representations*, pages 1–22, 2025. 2, 6, 1
- [43] Atsuyuki Miyai, Qing Yu, Go Irie, and Kiyoharu Aizawa. Locoop: Few-shot out-of-distribution detection via prompt learning. In *Annual Conference on Neural Information Processing Systems*, pages 76298–76310, 2023. 1, 3, 6, 7
- [44] Yuval Netzer, Tao Wang, Adam Coates, Alessandro Bissacco, Bo Wu, and Andrew Y. Ng. Reading digits in natural images with unsupervised feature learning. In *NIPS Workshop on Deep Learning and Unsupervised Feature Learning*, 2011. 2, 3
- [45] Anh Mai Nguyen, Jason Yosinski, and Jeff Clune. Deep neural networks are easily fooled: High confidence predictions for unrecognizable images. In *IEEE/CVF Conference on Computer Vision and Pattern Recognition*, pages 427–436, 2015. 1, 3
- [46] Jun Nie, Yonggang Zhang, Zhen Fang, Tongliang Liu, Bo Han, and Xinmei Tian. Out-of-distribution detection with negative prompts. In *International Conference on Learning Representations*, pages 1–20, 2024. 1, 3, 6
- [47] Alec Radford, Jong Wook Kim, Chris Hallacy, Aditya Ramesh, Gabriel Goh, Sandhini Agarwal, Girish Sastry, Amanda Askell, Pamela Mishkin, Jack Clark, Gretchen Krueger, and Ilya Sutskever. Learning transferable visual models from natural language supervision. In *International Conference on Machine Learning*, pages 8748–8763, 2021. 1, 2, 3, 5
- [48] Jie Ren, Peter J. Liu, Emily Fertig, Jasper Snoek, Ryan Poplin, Mark A. DePristo, Joshua V. Dillon, and Balaji Lakshminarayanan. Likelihood ratios for out-of-distribution detection.

- In *Annual Conference on Neural Information Processing Systems*, pages 14680–14691, 2019. 3
- [49] Jie Ren, Stanislav Fort, Jeremiah Z. Liu, Abhijit Guha Roy, Shreyas Padhy, and Balaji Lakshminarayanan. A simple fix to mahalanobis distance for improving near-ood detection. *CoRR*, abs/2106.09022, 2021. 7
- [50] Mohammadreza Salehi, Hossein Mirzaei, Dan Hendrycks, Yixuan Li, Mohammad Hossein Rohban, and Mohammad Sabokrou. A unified survey on anomaly, novelty, open-set, and out-of-distribution detection: Solutions and future challenges. *Trans. Mach. Learn. Res.*, 2022. 1
- [51] Yiyu Sun, Chuan Guo, and Yixuan Li. React: Out-of-distribution detection with rectified activations. In *Annual Conference on Neural Information Processing Systems*, pages 144–157, 2021. 3, 7
- [52] Yiyu Sun, Yifei Ming, Xiaojin Zhu, and Yixuan Li. Out-of-distribution detection with deep nearest neighbors. In *International Conference on Machine Learning*, pages 20827–20840, 2022. 3, 6, 2
- [53] Xinyu Tian, Shu Zou, Zhaoyuan Yang, and Jing Zhang. Argue: Attribute-guided prompt tuning for vision-language models. In *Conference on Computer Vision and Pattern Recognition*, pages 28578–28587, 2023. 6
- [54] Ashish Vaswani, Noam Shazeer, Niki Parmar, Jakob Uszkor-eit, Llion Jones, Aidan N. Gomez, Lukasz Kaiser, and Illia Polosukhin. Attention is all you need. In *Annual Conference on Neural Information Processing Systems*, pages 5998–6008, 2017. 3, 5
- [55] Sagar Vaze, Kai Han, Andrea Vedaldi, and Andrew Zisserman. Open-set recognition: A good closed-set classifier is all you need. In *International Conference on Learning Representations*, pages 1–27, 2022. 1, 5
- [56] Haoqi Wang, Zhizhong Li, Litong Feng, and Wayne Zhang. Vim: Out-of-distribution with virtual-logit matching. In *Conference on Computer Vision and Pattern Recognition*, pages 4911–4920, 2022. 3, 6, 1, 5
- [57] Hualiang Wang, Yi Li, Hui Feng Yao, and Xiaomeng Li. CLIPN for zero-shot OOD detection: Teaching CLIP to say no. In *International Conference on Computer Vision*, pages 1802–1812, 2023. 3, 6
- [58] Wei Wang, Tianhao Ma, Ming-Kun Xie, Gang Niu, and Masashi Sugiyama. Rethinking consistent multi-label classification under inexact supervision. In *International Conference on Learning Representations*, pages 1–26, 2026. 1
- [59] Yimu Wang, Evelien Riddell, Adrian Chow, Sean Sedwards, and Krzysztof Czarnecki. Mitigating the modality gap: Few-shot out-of-distribution detection with multi-modal prototypes and image bias estimation. *CoRR*, abs/2502.00662, 2025. 1, 3, 6
- [60] Zitai Wang, Qianqian Xu, Zhiyong Yang, Yuan He, Xiaochun Cao, and Qingming Huang. Openauc: towards auc-oriented open-set recognition. In *Annual Conference on Neural Information Processing Systems*, pages 25033–25045, 2022. 1
- [61] Zitai Wang, Qianqian Xu, Zhiyong Yang, Yuan He, Xiaochun Cao, and Qingming Huang. A unified generalization analysis of re-weighting and logit-adjustment for imbalanced learning. In *Annual Conference on Neural Information Processing Systems*, pages 48417–48430, 2023. 7
- [62] Zitai Wang, Qianqian Xu, Zhiyong Yang, Zhikang Xu, Linchao Zhang, Xiaochun Cao, and Qingming Huang. A unified perspective for loss-oriented imbalanced learning via localization. *IEEE Trans. Pattern Anal. Mach. Intell.*, 48(1):639–656, 2026. 7
- [63] Jianxiong Xiao, James Hays, Krista A. Ehinger, Aude Oliva, and Antonio Torralba. SUN database: Large-scale scene recognition from abbey to zoo. In *Conference on Computer Vision and Pattern Recognition*, pages 3485–3492, 2010. 5
- [64] Zhisheng Xiao, Qing Yan, and Yali Amit. Likelihood regret: An out-of-distribution detection score for variational auto-encoder. In *Annual Conference on Neural Information Processing Systems*, pages 20685–20696, 2020. 3
- [65] Kai Xu, Rongyu Chen, Gianni Franchi, and Angela Yao. Scaling for training time and post-hoc out-of-distribution detection enhancement. In *International Conference on Learning Representations*, pages 1–14, 2024. 7, 2
- [66] Jing Kang Yang, Pengyun Wang, Dejian Zou, Zitang Zhou, Kunyuan Ding, Wenxuan Peng, Haoqi Wang, Guangyao Chen, Bo Li, Yiyu Sun, Xuefeng Du, Kaiyang Zhou, Wayne Zhang, Dan Hendrycks, Yixuan Li, and Ziwei Liu. Openood: Benchmarking generalized out-of-distribution detection. In *Annual Conference on Neural Information Processing Systems*, pages 32598–32611, 2022. 2, 7, 5
- [67] Jing Kang Yang, Kaiyang Zhou, Yixuan Li, and Ziwei Liu. Generalized out-of-distribution detection: A survey. *Int. J. Comput. Vis.*, 132(12):5635–5662, 2024. 1, 3
- [68] Zhiyong Yang, Qianqian Xu, Zitai Wang, Sicong Li, Boyu Han, Shilong Bao, Xiaochun Cao, and Qingming Huang. Harnessing hierarchical label distribution variations in test agnostic long-tail recognition. In *International Conference on Machine Learning*, pages 56624–56664, 2024. 7
- [69] Zhiyong Yang, Qianqian Xu, Sicong Li, Zitai Wang, Xiaochun Cao, and Qingming Huang. Dirmix: Harnessing test agnostic long-tail recognition with hierarchical label variations. *IEEE Trans. Pattern Anal. Mach. Intell.*, pages 1–18, 2025. 7
- [70] Fanhu Zeng, Zhen Cheng, Fei Zhu, and Xu-Yao Zhang. Local-prompt: Extensible local prompts for few-shot out-of-distribution detection. In *International Conference on Learning Representations*, pages 1–18, 2025. 6
- [71] Boxuan Zhang, Jianing Zhu, Zengmao Wang, Tongliang Liu, Bo Du, and Bo Han. What if the input is expanded in OOD detection? In *Annual Conference on Neural Information Processing Systems*, pages 21289–21329, 2024. 6
- [72] Hai Zhang, Hang Yu, Junqiao Zhao, Di Zhang, Chang Huang, Hongtu Zhou, Xiao Zhang, and Chen Ye. How to fine-tune the model: unified model shift and model bias policy optimization. In *Annual Conference on Neural Information Processing Systems*, pages 59252–59272, 2023. 1
- [73] Jingyang Zhang, Jing Kang Yang, Pengyun Wang, Haoqi Wang, Yueqian Lin, Haoran Zhang, Yiyu Sun, Xuefeng Du, Kaiyang Zhou, Wayne Zhang, Yixuan Li, Ziwei Liu, Yiran Chen, and Hai Li. Openood v1.5: Enhanced benchmark for out-of-distribution detection. *CoRR*, abs/2306.09301, 2023. 2, 7, 5

- [74] Yabin Zhang and Lei Zhang. Adaneg: Adaptive negative proxy guided OOD detection with vision-language models. In *Annual Conference on Neural Information Processing Systems*, pages 38744–38768, 2024. [1](#), [2](#), [3](#), [4](#), [6](#), [7](#), [5](#)
- [75] Yabin Zhang, Wenjie Zhu, Chenhang He, and Lei Zhang. LAPT: label-driven automated prompt tuning for OOD detection with vision-language models. In *European Conference on Computer Vision*, pages 271–288, 2024. [6](#), [7](#)
- [76] Zhe Zhao, Pengkun Wang, Haibin Wen, Wei Xu, Lai Song, Qingfu Zhang, and Yang Wang. Two fists, one heart: Multi-objective optimization based strategy fusion for long-tailed learning. In *International Conference on Machine Learning*, pages 61040–61071, 2024. [7](#)
- [77] Bolei Zhou, Àgata Lapedriza, Aditya Khosla, Aude Oliva, and Antonio Torralba. Places: A 10 million image database for scene recognition. *IEEE Trans. Pattern Anal. Mach. Intell.*, 40(6):1452–1464, 2018. [2](#), [3](#), [5](#)
- [78] Shu Zou, Xinyu Tian, Qinyu Zhao, Zhaoyuan Yang, and Jing Zhang. Simlabel: Consistency-guided ood detection with pretrained vision-language models. In *Australasian Joint Conference on Artificial Intelligence*, page 110–121, 2025. [6](#)

Appendix

A. Pseudo-code for Modality Inversion

Here, we provide the pseudo-code for the modality inversion process in Algorithm 2. This procedure aims to transform a high-confidence OOD image into an extra negative text embedding by optimizing a set of pseudo-tokens.

Algorithm 2 Modality Inversion From Image To Text [42]

Require: High-confidence OOD image x , number of pseudo-tokens T , number of optimization steps S ;

- 1: Initialize $v = \{v_1, v_2, \dots, v_T\}$;
 - 2: Extract image embedding $h = \mathcal{I}(x)$;
 - 3: **for** $s = 1$ to S **do**
 - 4: Form $\bar{v} = [\mathcal{E}(\text{"a photo of"}), v]$;
 - 5: Extract text embedding $e_v^- = \mathcal{T}(\bar{v})$;
 - 6: Calculate the cosine loss $\mathcal{L} = 1 - \text{cos}(e_v^-, h)$;
 - 7: Update v to minimize \mathcal{L} ;
 - 8: **end for**
 - 9: **return** Negative text embedding $e_v^- = \mathcal{T}(\bar{v})$.
-

B. Additional Results

B.1. Full results on the OpenOOD Benchmark

Table 4. Full results of our method with ID dataset of ImageNet-1K on the OpenOOD benchmark.

Near / Far OOD	Datasets	FPR95 ↓	AUROC ↑
Near-OOD	SSB-hard [55]	69.96	80.24
	NINCO [3]	60.90	84.16
	Mean	65.43	82.20
Far-OOD	iNaturalist [24]	0.40	99.71
	Textures [7]	18.17	96.74
	OpenImage-O [56]	32.30	93.69
	Mean	16.96	96.71

B.2. Impact of ID/OOD Dataset Ordering.

To evaluate the robustness of our method to ID/OOD dataset ordering, we generate different dataset permutations by varying random seeds. As shown in Table 5, our method maintains stable performance with standard deviations of merely 0.05 (Four-OOD) and 0.46 (Near-OOD), demonstrating strong insensitivity to ordering effects.

Table 5. Average results of AUROC (↑) with five different seeds on both Four-OOD and Near-OOD benchmarks.

Benchmark	Seed					Mean	Std
	0	1	2	3	4		
Four-OOD	97.43	97.38	97.38	97.45	97.51	97.43	0.05
Near-OOD	82.20	81.56	81.50	82.29	82.59	82.03	0.46

B.3. More Results on the OpenOOD Benchmark

Following AdaNeg, we also evaluate our method on small-scale datasets from the OpenOOD benchmark. Specifically, we adopt CIFAR-10/100 [30] as an ID dataset while utilizing CIFAR-100/10 along with TinyImageNet (TIN) [31] as Near-OOD

Table 6. OOD detection results with ID dataset of CIFAR100 on the OpenOOD benchmark using CLIP ViT-B/16 architecture. Full results are available in Table 7.

Methods	FPR95 ↓		AUROC ↑	
	Near-OOD	Far-OOD	Near-OOD	Far-OOD
Methods requiring training on ID or extra data				
GEN [38]	–	–	81.31	79.68
VOS [13] + EBO [37]	–	–	80.93	81.32
SCALE [65]	–	–	80.99	81.42
OE [21] + MSP [20]	–	–	88.30	81.41
Zero-shot methods (no training on ID or extra data)				
MCM [41]	75.20	59.32	71.00	76.00
NegLabel [29]	71.44	40.92	70.58	89.68
AdaNeg [74]	59.07	29.35	84.60	95.25
InterNeg	62.54	20.02	85.45	96.39

Table 7. Full results of our method with ID dataset of CIFAR100 on the OpenOOD benchmark.

Near / Far OOD	Datasets	FPR95 ↓	AUROC ↑
Near-OOD	CIFAR100 [30]	60.10	84.19
	TIN [31]	64.99	86.71
	Mean	62.54	85.45
Far-OOD	MNIST [9]	0.01	99.97
	SVHN [44]	3.23	99.41
	Texture [7]	21.16	96.84
	Places365 [77]	55.68	89.36
	Mean	20.02	96.39

Table 8. OOD detection results with ID dataset of CIFAR10 on the OpenOOD benchmark using CLIP ViT-B/16 architecture. Full results are available in Table 9.

Methods	FPR95 ↓		AUROC ↑	
	Near-OOD	Far-OOD	Near-OOD	Far-OOD
Methods requiring training on ID or extra data				
PixMix [23] + KNN [52]	–	–	93.10	95.94
OE [21] + MSP [20]	–	–	94.82	96.00
PixMix [23] + RotPred [22]	–	–	94.86	98.18
Zero-shot methods (no training on ID or extra data)				
MCM [41]	30.86	17.99	91.92	95.54
NegLabel [29]	28.75	6.60	94.58	98.39
AdaNeg [74]	20.40	2.79	94.78	99.26
InterNeg	23.93	2.59	95.13	99.29

datasets. For Far-OOD datasets, we consider MNIST [9], SVHN [44], Texture [7], and Places365 [77]. For hyperparameters, we maintain consistency with the experimental setup described in Section C, modifying only M (set to 70,000) to align with AdaNeg and ensure fair comparison. All other parameters remain unchanged. In the Near-OOD setting, our method achieves the best results on the AUROC metric.

As illustrated in Table 6 and Table 8, our method still achieves state-of-the-art performance in the Far-OOD setting, even outperforming those training methods.

Table 9. Full results of our method with ID dataset of CIFAR10 on the OpenOOD benchmark.

Near / Far OOD	Datasets	FPR95 ↓	AUROC ↑
Near-OOD	CIFAR100 [30]	37.26	91.81
	TIN [31]	10.60	98.45
	Mean	23.93	95.13
Far-OOD	MNIST [9]	0.00	100.00
	SVHN [44]	0.06	99.97
	Texture [7]	0.41	99.57
	Places365 [77]	9.89	97.61
	Mean	2.59	99.29

B.4. Ablation of Different CLIP Architectures

As shown in Table 10, we evaluate multiple CLIP backbone architectures in the Four-OOD setting using ImageNet-1K as the ID dataset. The experimental results demonstrate that our method consistently outperforms all baseline approaches by a substantial margin across different backbone architectures. This robust performance advantage highlights both the effectiveness and robustness of our proposed method.

Table 10. OOD detection results with ID dataset of ImageNet-1k and traditional Four-OOD datasets using different CLIP backbone architectures.

Backbones	Methods	OOD Datasets								Average	
		iNaturalist		SUN		Places		Textures		AUROC↑	FPR95↓
		AUROC↑	FPR95↓	AUROC↑	FPR95↓	AUROC↑	FPR95↓	AUROC↑	FPR95↓	AUROC↑	FPR95↓
ResNet50	NegLabel	99.24	2.88	94.54	26.51	89.72	42.60	88.40	50.80	92.97	30.70
	CSP	99.46	1.95	95.73	19.05	90.39	38.58	92.41	32.66	94.50	23.06
	AdaNeg	99.58	1.18	97.37	10.56	93.84	43.19	94.18	35.00	96.24	22.48
	InterNeg	99.56	1.16	98.35	7.99	93.71	37.82	96.05	21.92	96.92	17.22
ResNet101	NegLabel	99.27	3.11	94.96	24.55	89.42	44.82	87.22	52.78	92.72	31.32
	CSP	99.47	2.04	95.71	19.50	90.27	39.57	90.59	38.67	94.01	24.95
	AdaNeg	99.69	0.78	97.65	10.61	94.00	40.38	93.59	39.44	96.23	22.80
	InterNeg	99.64	0.87	98.54	7.02	93.70	38.32	95.94	24.74	96.96	17.74
ViT-B/32	NegLabel	99.11	3.73	95.27	22.48	91.72	34.94	88.57	50.51	93.67	27.92
	CSP	99.46	2.37	96.49	15.01	92.42	31.47	93.64	25.09	95.50	18.49
	AdaNeg	99.67	0.87	97.74	9.62	93.98	36.45	94.58	33.26	96.49	20.05
	InterNeg	99.68	0.70	98.74	5.79	93.65	38.05	96.02	23.55	97.02	17.02
ViT-B/16	NegLabel	99.49	1.91	95.49	20.53	91.64	35.59	90.22	43.56	94.21	25.40
	CSP	99.61	1.54	96.69	13.82	92.85	29.69	93.78	25.78	95.73	17.71
	AdaNeg	99.71	0.59	97.44	9.50	94.55	34.34	94.93	31.27	96.66	18.93
	InterNeg	99.79	0.40	98.68	6.78	95.01	27.11	96.26	21.85	97.43	14.04
ViT-L/14	NegLabel	99.53	1.77	95.63	22.33	93.01	32.22	89.71	42.92	94.47	24.81
	CSP	99.72	1.21	96.73	14.88	93.58	28.41	92.71	28.16	95.69	18.17
	AdaNeg	99.82	0.26	97.97	7.94	95.12	28.67	94.24	38.28	96.79	18.79
	InterNeg	99.88	0.21	98.75	5.88	95.03	26.82	96.07	22.89	97.43	13.95

B.5. Cross-Domain Analysis

In cross-domain settings, there is usually no ID training set provided for constructing ID image proxies. To evaluate our method in a cross-domain scenario, we conduct two additional experiments as follows:

- **ImageNet ID Image Proxies:** Since ImageNet-V2 is a variant of ImageNet, we use the image proxies computed from the original ImageNet training set as a substitute.
- **ImageNet-V2 ID Image Proxies:** Alternatively, we randomly select a small subset of ID images (e.g., 4 images per class) from ImageNet-V2 itself to compute the ID image proxies, and use the rest for testing.

Specifically, we set ImageNet-V2 as the ID dataset and Four-OOD (iNaturalist, SUN, Places, Textures) as the OOD datasets. Table 11 shows the average results across the Four-OOD datasets. These results demonstrate that our method remains effective and robust in cross-domain scenarios.

Table 11. Cross-domain OOD detection performance on ImageNet-V2 with Four-OOD datasets.

ID Image Proxies Source	Method	AUROC \uparrow	FPR95 \downarrow
ImageNet	NegLabel	93.08	29.77
	AdaNeg	96.24	19.21
	Ours	96.84	18.40
ImageNet-V2	NegLabel	93.90	27.64
	AdaNeg	96.19	19.97
	Ours	96.96	18.18

B.6. ID Misclassification with Different OOD Datasets

Since both AdaNeg and our method dynamically adjust the OOD score according to the test images during inference, it is important to evaluate additional OOD datasets to better understand the phenomenon of ID misclassification. In Figure 2, we use SUN as the OOD dataset. Here, we extend the evaluation to other OOD datasets included in the Four-OOD benchmark. As shown in Figure 5, our method consistently outperforms AdaNeg across various OOD datasets, demonstrating the robustness and effectiveness of InterNeg.

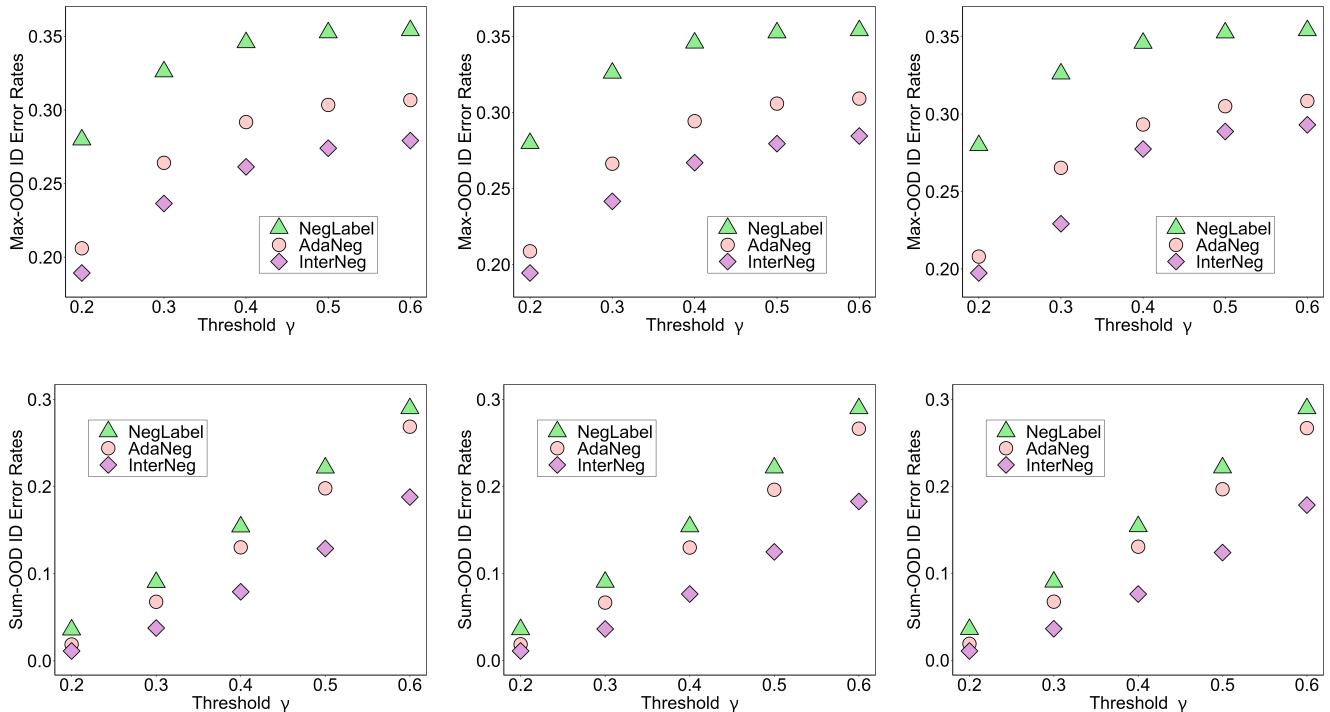


Figure 5. Max-OOD and Sum-OOD ID error rates on different OOD datasets. *Left:* iNaturalist. *Middle:* Places. *Right:* Textures.

B.7. Inference Cost

We evaluate the inference efficiency of our approach on the traditional Four-OOD benchmark, using ImageNet-1K as the ID dataset (see Table 12). When measured on an NVIDIA RTX 3090 GPU, our method incurs only a **minor** computational overhead compared to AdaNeg.

Method	Mean	iNaturalist	Places	Textures	SUN
AdaNeg	0.0058	0.0068	0.0046	0.0093	0.0025
Ours	0.0067	0.0074	0.0055	0.0113	0.0029

Table 12. Comparison of inference time (seconds per image).

B.8. Sensitivity to Corpus Choice

To investigate the impact of the underlying corpus, we substitute WordNet with the Common-20K and Part-of-Speech corpora. As shown in Table 13, our method consistently outperforms the strongest baseline, AdaNeg, reducing the average FPR95 by **3.62%** and **4.76%**, respectively. This demonstrates that our performance improvements are robust and agnostic to the choice of the source corpus.

Source	Method	Average	
		AUROC \uparrow	FPR95 \downarrow
Common-20K	NegLabel	90.50	43.02
	CSP	92.06	36.56
	AdaNeg	93.12	32.39
	Ours	94.58	28.77
Part-of-Speech	NegLabel	92.71	32.12
	CSP	94.21	24.42
	AdaNeg	95.07	23.17
	Ours	95.98	18.41

Table 13. Evaluation with different corpus sources on the traditional Four-OOD benchmark, using ImageNet-1K as the ID dataset.

C. Experimental Setup

Datasets. Following previous work [6, 16, 29, 74], we evaluate our method on the large-scale ImageNet-1K Four-OOD detection benchmark [27]. This widely-used benchmark utilizes the ImageNet-1K [8] dataset as ID data and iNaturalist [24], SUN [63], Places [77], Textures [7] as four OOD datasets, where the labels of the four OOD datasets that overlap with ImageNet-1K have been manually removed. Furthermore, we also conduct experiments on the OpenOOD benchmark [66, 73] following [74]. This benchmark also uses ImageNet-1K as the ID dataset, while categorizing OOD data into two distinct groups based on the empirical performance of OOD detectors: Near-OOD (*e.g.*, SSB-hard [55], NINCO [3]) and Far-OOD (*e.g.*, iNaturalist [24], Textures [7], OpenImage-O [56]). Also, each OOD dataset has no classes that overlap with the ID dataset.

Implementation Details. In this paper, we implement various CLIP [47] backbone architectures, including ResNet50, ResNet101, ViT-B/32, ViT-B/16 and ViT-L/14. Unless otherwise specified, we adopt the CLIP ViT-B/16 model as the pre-trained VLM, which consists of a visual encoder based on ViT-B/16 Vision Transformer [11] and a text encoder built on Text Transformer [54]. For hyperparameters, we set the number N of ID images per class as 16, the number M of negative texts as 2000, the maximum size K of extra negative text embeddings as 2000, temperature $\tau = 1.0$ and threshold $\beta = 0.35$ in all experiments. Following [29, 47], we employ the text prompt template of "The nice [class]". All experiments are conducted using NVIDIA RTX 3090 GPUs.

Evaluation Metrics. Following common practice [6, 16, 29, 74], we adopt the following metrics to evaluate the OOD detection performance: (1) AUROC, the area under the receiver operating characteristic curve; (2) FPR95, the false positive rate of the OOD data when the true positive rate of ID data is 95%.

D. Comparison with ArGue and SimLabel.

It is crucial to distinguish our approach from recent methods such as SimLabel [78] and ArGue [53]. First, we differentiate our focus on **metric consistency**—aligning the OOD detection metric with CLIP’s inter-modal training objective—from SimLabel’s **semantic consistency**, which focuses on aligning ID labels with semantic synonyms. Second, our method and ArGue **differ fundamentally** in their core paradigms. ArGue employs prompt tuning with negative attributes to suppress spurious visual features, aiming for robust ID classification. In contrast, InterNeg leverages inter-modal guided negative texts explicitly tailored for OOD detection.

E. Clarification on Zero-Shot OOD Detection and ID Data Dependency

Definition of Zero-Shot OOD Detection. In the context of Out-of-Distribution (OOD) detection, we align our setting with the established consensus in prior literature. For instance, NegLabel defines the zero-shot capability as predicting the correct label “*without prior training on that specific class.*” Similarly, EOE characterizes it as operating “*without re-training on any unseen ID data.*” Therefore, the term “zero-shot” typically describes the training pipeline, especially for the CLIP module. Given this constraint, it is a common practice for the baselines in this field to introduce external knowledge or additional modules. For example, ZOC /CLIPN trains a captioner/encoder to generate candidate unknown classes/negative semantics within images, respectively. To mitigate the training burden, recent advances such as NegLabel and AdaNeg turn to proxies to enhance the representations of potential OOD classes. Our method **follows this paradigm** by fixing the fundamental inconsistency hidden in the proxy generation, **without training on either ID or external data.**

Dependency on ID Data. Furthermore, assuming access to a small set of ID data is highly realistic for real-world OOD detection deployments (e.g., autonomous driving and medical diagnosis), where ID classes are inherently known and well-defined. Crucially, in our framework, we utilize ID samples **solely for proxy calculation, not model training.** As validated in Figure 4, our approach achieves state-of-the-art performance with a minimal ID data dependency of merely 4 images per class, underscoring its practical applicability.